



## Photoelectron spectroscopic study of iron–benzene cluster anions

Weijun Zheng<sup>a</sup>, Soren N. Eustis<sup>a</sup>, Xiang Li<sup>a</sup>, John M. Nilles<sup>a</sup>, Owen C. Thomas<sup>a</sup>, Kit H. Bowen<sup>a,\*</sup>, Anil K. Kandalam<sup>b</sup>

<sup>a</sup>Departments of Chemistry and Material Sciences, Johns Hopkins University, 3400 N Charles street, Baltimore, MD 21218, United States

<sup>b</sup>Department of Physics, McNeese State University, Lake Charles, LA 70609, United States

### ARTICLE INFO

#### Article history:

Received 24 June 2008

In final form 14 July 2008

Available online 22 July 2008

### ABSTRACT

Iron–benzene cluster anions,  $\text{Fe}_n\text{Bz}_m^-$  ( $n = 1-7$ ,  $m = 1-4$ ), were generated via laser vaporization and studied using mass spectrometry, anion photoelectron spectroscopy and in one case by density functional theory. Based on these studies, we propose that  $\text{Fe}_1\text{Bz}_1^-$  and  $\text{Fe}_1\text{Bz}_1$  as well as  $\text{Fe}_2\text{Bz}_1^-$  and  $\text{Fe}_2\text{Bz}_1$  exhibit half-sandwich structures, that  $\text{Fe}_1\text{Bz}_2^-$  and  $\text{Fe}_1\text{Bz}_2$ ,  $\text{Fe}_2\text{Bz}_2^-$  and  $\text{Fe}_2\text{Bz}_2$ , as well as  $\text{Fe}_3\text{Bz}_2$  and  $\text{Fe}_4\text{Bz}_2$  are sandwich structures, and that  $\text{Fe}_2\text{Bz}_3^-$  and  $\text{Fe}_2\text{Bz}_3$  and larger species form ‘rice-ball’ structures which in each case consist of benzene molecules surrounding an iron cluster core.

© 2008 Elsevier B.V. All rights reserved.

### 1. Introduction

The bonding in transition metal–organic molecular complexes is dominated by d-electron/ $\pi$ -electron interactions. Recently, transition metal–organic complexes have received attention due to their potential as building blocks for novel magnetic and/or hydrogen storage materials [1–3]. Transition metal complexes with benzene are the simplest transition metal–organic complexes in which the organic moiety is aromatic. Transition metal–benzene complexes/clusters have been studied by collision-induced dissociation [4,5], photodissociation [6,7], photoionization [8–10], photoelectron spectroscopy [11–16], electric deflection [17], and theory [18–27]. Nakajima, Kaya, and coworkers [8] showed that transition metal–benzene complexes form either multiple-decker sandwich structures or ‘rice-ball’ structures, based on the number of d-electrons in their transition metals. In ‘rice-ball’ structures, a metal cluster core is surrounded by organic ligands. They found that the early transition metals tended to form multiple-decker sandwich structures with benzene molecules, while the late transition metals tended to form ‘rice-ball’ structures with benzene.

The iron–benzene cluster system is the subject of this report. A number of studies have been performed on these systems. These include photoionization experiments on neutral iron–benzene clusters by Nakajima, Kaya, and coworkers [8], photodissociation studies on cationic iron–benzene clusters by Duncan and coworkers [6,7], theoretical investigations on the  $\text{Fe}_1\text{Bz}_1$  cation by Bauschlicher [18] and Klippenstein and coworkers [26,27], and  $\text{Fe}_1\text{Bz}_1$ ,  $\text{Fe}_1\text{Bz}_2$  and their anions by Pandey, Jena, and coworkers [24,25]. Here, we report the mass spectrum and negative ion photoelectron spectra of the  $\text{Fe}_n\text{Bz}_m^-$  ( $n = 1-7$ ,  $m = 1-4$ ) cluster anion

series. We have also conducted theoretical calculations on the  $\text{Fe}_1\text{Bz}_1^-/\text{Fe}_1\text{Bz}_1$  system. Based on our results, as well as evidence from previous work, we propose structures for these  $\text{Fe}_n\text{Bz}_m^-$  cluster anions.

### 2. Methods

#### 2.1. Experimental

Negative ion photoelectron spectroscopy is conducted by crossing a mass-selected beam of anions with a fixed frequency photon beam and energy analyzing the resultant photodetached electrons. This technique is governed by the energy-conserving relationship  $h\nu = \text{EKE} + \text{EBE}$ , where  $h\nu$  is the photon energy, EKE is the measured electron kinetic energy, and EBE is the electron binding energy. The details of our apparatus have been described elsewhere [28]. Briefly, both mass spectra and anion photoelectron (photodetachment) spectra were collected on an apparatus consisting of a laser vaporization source, a linear time-of-flight mass spectrometer for mass analysis and selection (resolution  $\sim 1000$ ), and a magnetic bottle photoelectron spectrometer for electron energy analysis (resolution is  $\sim 35$  meV at 1 eV EKE). The third harmonic (355 nm, 3.493 eV/photon) of a Nd:YAG laser was used to photodetach electrons from the cluster anions of interest. Photoelectron spectra were calibrated against the well known atomic lines of the copper anion [29].  $\text{Fe}_n(\text{Bz})_m^-$  cluster anions were generated in this experiment in a laser vaporization source consisting of a rotating, translating iron rod (6.3 mm diameter, Aldrich Chem. Co., purity 99.98%) which was ablated with second harmonic (532 nm) light pulses from a Nd:YAG laser, while  $\sim 4$  atm. of helium gas seeded with benzene vapor was expanded from a pulsed valve over the iron rod.

\* Corresponding author. Fax: +1 410 516 8420.

E-mail address: [kbowen@jhu.edu](mailto:kbowen@jhu.edu) (K.H. Bowen).

## 2.2. Computational

Theoretical calculations were performed using the mPW1PW91 functional [30] and the 6-31+G(d,p) basis set for all atoms. Ground state structures for the anionic and neutral species were determined by optimizing structures at several different multiplicities using several different starting geometries. Optimizations were not symmetry constrained. Adiabatic electron affinities ( $EA_a$ ) were calculated as the energy difference between the ground states of the neutral and anionic species. Photodetachment transitions were calculated as the difference between the ground state anion energy and the energy of the corresponding neutral frozen at the geometry of the anion for each possible spin state, these being governed by  $\Delta(\text{spin multiplicity}) = \pm 1$ . All calculations were performed with GAUSSIAN 03 [31] and visualized with ChemCraft [32]. Our theoretical findings are presented in Section 4, where we discuss the one system that we studied computationally.

## 3. Results

### 3.1. Mass spectra

Fig. 1 shows a typical, reproducible mass spectrum of the  $Fe_nBz_m^-$  cluster anions generated in this study. The mass spectrum of this system is much richer than those which we observed previously in our studies of the cobalt–benzene [11], titanium–benzene [14], and nickel–benzene [15] cluster anion systems. Interestingly, in the mass spectrum of  $Fe_nBz_m^-$ ,  $m$  was always smaller than  $n+2$ . For example,  $Fe_1Bz_3^-$ ,  $Fe_2Bz_4^-$ , and  $Fe_3Bz_5^-$  were not seen in any of these experiments. We also observed that the  $Fe_nBz_m^-$  ion intensities became very weak when the number of benzene molecules exceeded four. The relative intensities of mass peaks provide information about the relative stabilities of the corresponding species. Especially intense mass peaks were observed for  $Fe_1Bz_2^-$ ,  $Fe_2Bz_2^-$ ,  $Fe_2Bz_3^-$ ,  $Fe_3Bz_3^-$ , and  $Fe_4Bz_4^-$ . Based on this observation, we suggest that  $Fe_1Bz_2^-$ ,  $Fe_2Bz_3^-$ ,  $Fe_3Bz_3^-$ , and  $Fe_4Bz_4^-$  all enjoy enhanced stabilities compared to their neighboring  $Fe_nBz_m^-$  compositions.

### 3.2. Photoelectron spectra

The photoelectron spectra of iron–benzene cluster anions measured with 3.493 eV photons are shown in Fig. 2. The spectra of the smaller iron–benzene clusters, such as  $Fe_1Bz_1^-$ ,  $Fe_2Bz_1^-$ ,  $Fe_1Bz_2^-$ , and

$Fe_2Bz_2^-$  are well structured, while those of larger iron–benzene clusters are broad and much less structured. Adiabatic electron affinities ( $EA_a$ ) were estimated from the threshold regions of the photoelectron spectra, in each case taking it to be the EBE of the onset plus an offset of  $\sim 0.2$  eV to account for the typical effect of hot bands. In cases where the lowest EBE peak showed a sharp rise in intensity, however, a smaller offset was utilized. The  $EA_a$  values of  $Fe_nBz_m^-$  clusters, estimated in this way, are presented in Table 1. In the following discussion, we have grouped the cluster compositions based on their proposed structural motifs.

## 4. Discussion

### 4.1. Half-sandwich structures ( $Fe_1Bz_1^-/Fe_1Bz_1$ and $Fe_2Bz_1^-/Fe_2Bz_1$ )

The spectrum of  $Fe_1Bz_1^-$  has four major peaks. The first and most intense peak is centered at  $EBE = 0.60$  eV. The other three peaks have lower intensities and are centered at  $EBE = 1.08$  eV, 1.30 eV, and 2.15 eV. We estimate the electron affinity of  $Fe_1Bz_1^-$  neutral to be 0.46 eV. The photoelectron spectrum of  $Fe_1Bz_1^-$  shows a strong similarity to the photoelectron spectrum of  $V_1Bz_1^-$  measured by Kaya, Nakajima, and coworkers [12]. The main difference between them is the fact that the peaks in the  $V_1Bz_1^-$  spectrum are all located at slightly higher electron binding energies. The electron affinity of  $V_1Bz_1$  is 0.62 eV as determined in their study. This suggests that the  $Fe_1Bz_1/Fe_1Bz_1^-$  system adopts structures which are similar to those of the  $V_1Bz_1/V_1Bz_1^-$  system, and that the interaction between an iron atom and benzene is also similar to that between a vanadium atom and benzene. According to Kaya, Nakajima, and coworkers, the  $V_1Bz_1^-$  anion prefers a half-sandwich structure with the vanadium atom sitting on top of the benzene ring. Also, the lowest EBE peak in the spectrum of  $V_1Bz_1^-$  corresponds to photodetachment from a non-bonding orbital. Thus, it is reasonable to conclude on this basis alone that  $Fe_1Bz_1^-$  has a similar half-sandwich structure, and that the lowest EBE peak in the spectrum of  $Fe_1Bz_1^-$  corresponds to photodetachment from a non-bonding orbital.

Our theoretical calculations showed both the neutral and anionic geometries of  $Fe_1Bz_1$  and  $Fe_1Bz_1^-$  to be fully symmetric  $C_{6v}$  structures (see Fig. 3), thus confirming the half-sandwich hypothesis. The fact that both the anion and the neutral have such similar structures is reflected in the narrowness of the lowest EBE peak in the photoelectron spectrum of  $Fe_1Bz_1^-$ , i.e., a narrow peak implies a high Franck–Condon overlap between the anion and its neutral. The  $EA_a$  value that we calculated for  $Fe_1Bz_1$  is 0.36 eV which is the energy of the transition from  $v'' = 0$  of the anion's (quartet) ground state to  $v' = 0$  of the corresponding neutral's (triplet) ground state. (A previous calculation had found the  $EA_a$  value for  $Fe_1Bz_1$  to be 0.01 eV [24].) Our calculated value is in reasonably good agreement with our experimental value of 0.46 eV. The vertical transition energies that we calculated for this system are at  $EBE = 0.41$  eV and 0.93 eV, i.e., transitions from the anion's ground state to the neutral's triplet and quintet states, respectively. These results also compare reasonably well with EBE values of the lowest and second lowest measured transition energies of 0.60 eV and 1.08 eV. Thus, we are satisfied that the proposed half-sandwich structure is correct. We also conducted calculations on several of the other  $Fe_nBz_m^-/Fe_nBz_m$  systems to be discussed below. Unfortunately, despite stringent efforts by ourselves and earlier by others, we were not able to achieve satisfactory agreement between theory and experiment for systems other than the present one in this series.

The spectrum of  $Fe_2Bz_1^-$  exhibits a peak centered at  $EBE = 1.26$  eV, several weaker peaks in the EBE range of 1.4–1.7 eV, and a strong, sharp peak at 2.53 eV. The electron affinity of  $Fe_2Bz_1$  was estimated to be 1.15 eV. The profiles of the photoelectron spectra of both  $Fe_2Bz_1^-$  and the earlier reported photoelectron

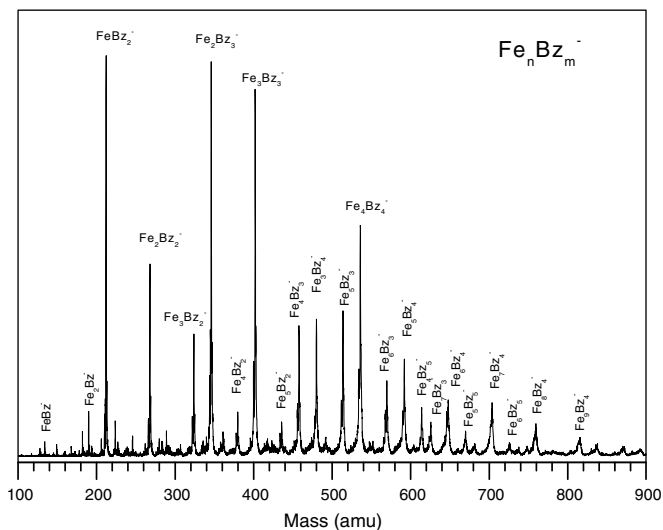


Fig. 1. Mass spectrum of iron–benzene cluster anions.

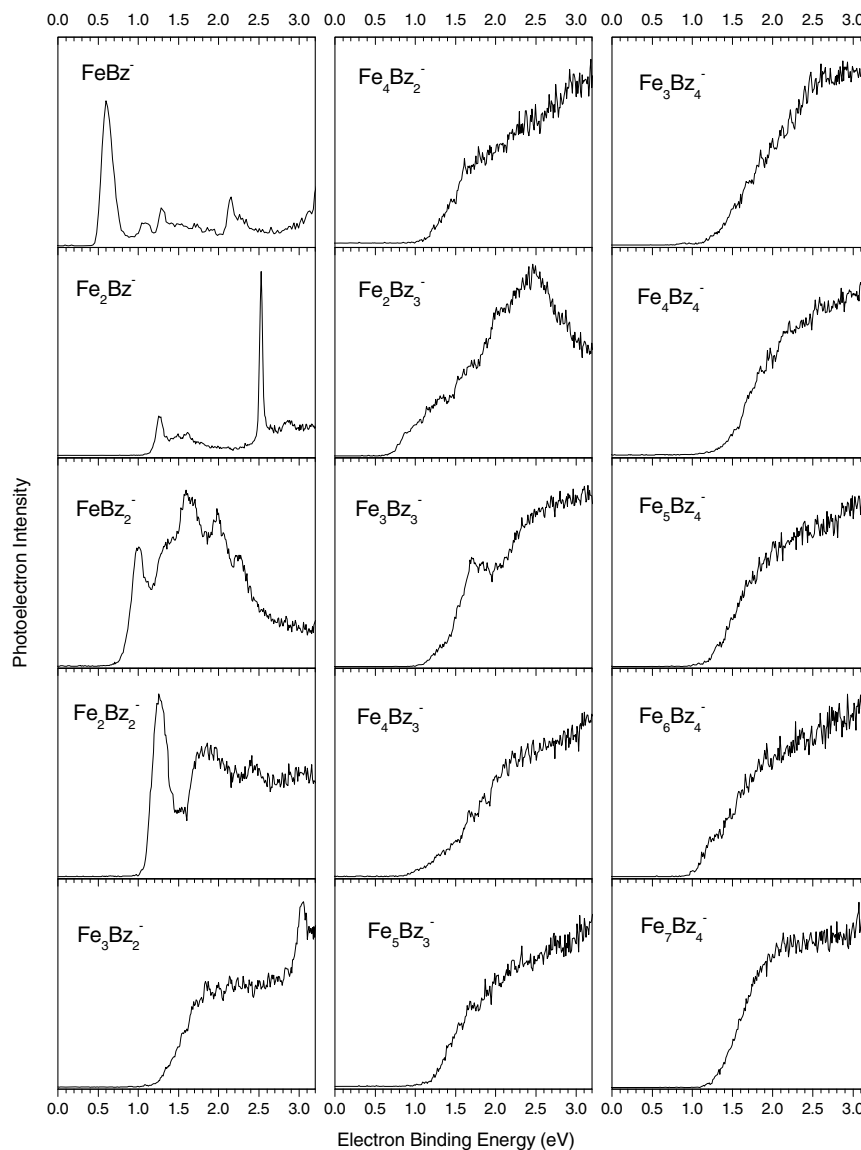


Fig. 2. Photoelectron spectra of iron–benzene cluster anions taken with 355 nm photons.

**Table 1**  
Estimated electron affinities of iron–benzene clusters (uncertainty =  $\pm 0.10$  eV)

Cluster	EA <sub>a</sub> (eV)	Cluster	EA <sub>a</sub> (eV)
FeBz	0.46	Fe <sub>4</sub> Bz <sub>3</sub>	1.1
Fe <sub>2</sub> Bz	1.15	Fe <sub>5</sub> Bz <sub>3</sub>	1.3
FeBz <sub>2</sub>	0.78	Fe <sub>3</sub> Bz <sub>4</sub>	1.4
Fe <sub>2</sub> Bz <sub>2</sub>	1.08	Fe <sub>4</sub> Bz <sub>4</sub>	1.4
Fe <sub>3</sub> Bz <sub>2</sub>	1.3	Fe <sub>5</sub> Bz <sub>4</sub>	1.3
Fe <sub>4</sub> Bz <sub>2</sub>	1.3	Fe <sub>6</sub> Bz <sub>4</sub>	1.1
Fe <sub>2</sub> Bz <sub>3</sub>	0.8	Fe <sub>7</sub> Bz <sub>4</sub>	1.4
Fe <sub>3</sub> Bz <sub>3</sub>	1.2		

spectrum of Fe<sub>2</sub>Cor<sub>1</sub><sup>-</sup> (Cor = coronene) [33] are quite similar but with their peak positions shifted slightly relative to one another. We therefore postulate that Fe<sub>2</sub>Bz<sub>1</sub><sup>-</sup> prefers the same structure as that found in Fe<sub>2</sub>Cor<sub>1</sub><sup>-</sup>. Our calculations for Fe<sub>2</sub>Cor<sub>1</sub><sup>-</sup> gave transition energies which agreed with those in our measured photoelectron spectrum of Fe<sub>2</sub>Cor<sub>1</sub><sup>-</sup> [33]. These calculations found a ground state structure for Fe<sub>2</sub>Cor<sub>1</sub><sup>-</sup> in which an iron dimer interacts with coron-

ene with the bond axis of the dimer perpendicular to the coronene plane. Thus, we propose that Fe<sub>2</sub>Bz<sub>1</sub><sup>-</sup> adopts the same half-sandwich structure. Anion photoelectron spectra reflect the properties of the anion's corresponding neutral as well as those of the anion. Our calculations on the Fe<sub>2</sub>Cor<sub>1</sub><sup>-</sup>/Fe<sub>2</sub>Cor<sub>1</sub> system found two almost degenerate isomers for neutral Fe<sub>2</sub>Cor<sub>1</sub>. One of the neutral isomers had the same perpendicular dimer axis structure found in the lowest energy Fe<sub>2</sub>Cor<sub>1</sub><sup>-</sup> anion, while the other one exhibited a structure with the iron dimer axis parallel to the plane of the coronene molecule. These structures are likely to be the same as those of neutral Fe<sub>2</sub>Bz.

#### 4.2. Sandwich structures (Fe<sub>1</sub>Bz<sub>2</sub><sup>-</sup>/Fe<sub>1</sub>Bz<sub>2</sub>, Fe<sub>2</sub>Bz<sub>2</sub><sup>-</sup>/Fe<sub>2</sub>Bz<sub>2</sub> plus Fe<sub>3</sub>Bz<sub>2</sub> and Fe<sub>4</sub>Bz<sub>2</sub>)

The photoelectron spectrum of Fe<sub>1</sub>Bz<sub>2</sub><sup>-</sup> has five distinguishable peaks centered at EBE = 1.00 eV, 1.33 eV, 1.62 eV, 1.98 eV, and 2.25 eV. We estimate the adiabatic electron affinity value of Fe<sub>1</sub>Bz<sub>2</sub> to be 0.78 eV. Pandey et al. carried out calculations on the Fe<sub>1</sub>Bz<sub>2</sub><sup>-</sup>/Fe<sub>1</sub>Bz<sub>2</sub> system in which they froze the geometry of Fe<sub>1</sub>Bz<sub>2</sub> in a D<sub>6h</sub> sandwich structure, finding its adiabatic electron affinity to be

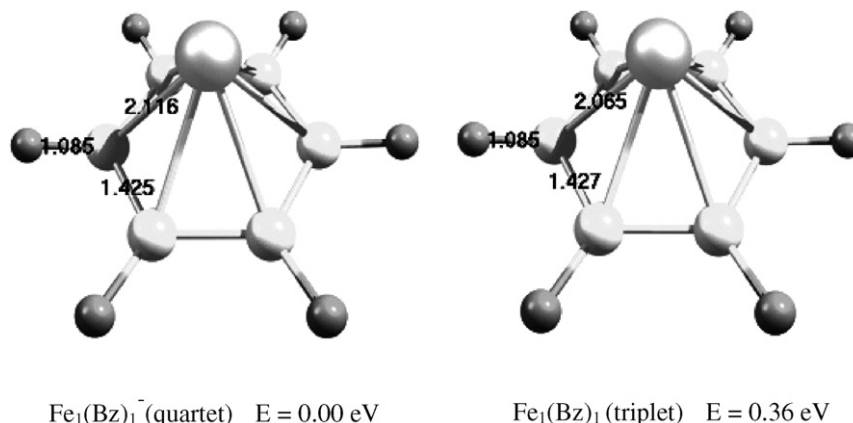


Fig. 3. Calculated ground state structures, energies, and bond lengths for the  $\text{Fe}_1(\text{Bz})_1$  neutral and its anion.

0.60 eV [25]. Based on the reasonably good agreement between their calculated  $EA_a$  value and our experimental value, we propose that neutral  $\text{Fe}_1\text{Bz}_2$  has a sandwich structure. Given the narrowness of the lowest energy (origin-containing) peak in the photoelectron spectrum of  $\text{Fe}_1\text{Bz}_2^-$ , it is likely that the  $\text{Fe}_1\text{Bz}_2^-$  anion also exhibits essentially the same structure, although there are no doubt differences in bond lengths and conceivably in the tilt of molecular planes.  $\text{Fe}_1\text{Bz}_2^-$  is the smallest cluster anion in this series to form a sandwich structure. The inherent stability of that structure may be the reason why it is especially abundant in the mass spectrum.

The photoelectron spectrum of  $\text{Fe}_2\text{Bz}_2^-$  has a strong peak centered at  $EBE = 1.25$  eV and two broad peaks at 1.85 eV and 2.40 eV. The electron affinity of  $\text{Fe}_2\text{Bz}_2$  is estimated to be 1.08 eV. There are three plausible possibilities for the structure of  $\text{Fe}_2\text{Bz}_2^-$ . They are  $|\cdot|$ ,  $|\cdot|$ , and  $|\cdot|$ . From our experience with the  $\text{Fe}_n(\text{Cor})_m^-$  system, we have seen that iron atoms tend to dimerize [33]. Thus, we speculate that an iron dimer is sandwiched between the two benzene molecules in one of the first two structures for  $\text{Fe}_2\text{Bz}_2^-$  shown schematically above. The orientation of the dimer axis relative to the benzene molecules, however, remains an open question. Its sandwich structure may also be the reason why  $\text{Fe}_2\text{Bz}_2^-$  also shows some enhanced abundance in the system's mass spectrum. Based on the narrowness of the lowest EBE peak in the photoelectron spectrum, the structure of neutral  $\text{Fe}_2\text{Bz}_2$  is probably the same as that of  $\text{Fe}_2\text{Bz}_2^-$  in general terms at least.

It would also seem reasonable to expect the structures of  $\text{Fe}_3\text{Bz}_2$  and  $\text{Fe}_4\text{Bz}_2$  to consist of aggregated iron trimers and tetramers each sandwiched between two benzene molecules. However, due to their broad spectral profiles and lack of narrow origin peaks, it is not clear whether both their anions and their neutrals share the same structures. Furthermore, the possibility of multiple isomers in the molecular beam cannot be overlooked.

#### 4.3. Rice-ball structures ( $\text{Fe}_2\text{Bz}_3^-/\text{Fe}_2\text{Bz}_3$ and the others)

Kaya, Nakajima, and coworkers found that late transition metals, such as iron, tend to form rice-ball structures with benzene [8]. This is also consistent with our observation that iron atoms tend to aggregate within iron/organic molecule complexes [33]. Thus, as these systems become compositionally more complex, with substantial numbers of both metal atoms and organic molecules, there is a tendency for their metal atoms to aggregate, forming cores (due to strong metal-metal bonding) around which their organic moieties build pseudo-shells.

In fact, the  $\text{Fe}_2\text{Bz}/\text{Fe}_2\text{Bz}^-$ ,  $\text{Fe}_2\text{Bz}_2/\text{Fe}_2\text{Bz}_2^-$ ,  $\text{Fe}_3\text{Bz}_2$ , and  $\text{Fe}_4\text{Bz}_2$  systems can all be considered to have incipient rice-ball structures.

They just do not have enough benzene molecules available to enclose their iron cluster 'cores'. However, once a third-benzene is added, as in  $\text{Fe}_2\text{Bz}_3$ ,  $\text{Fe}_3\text{Bz}_3$ , and  $\text{Fe}_4\text{Bz}_3$ , the rice-ball motif comes into play. We speculate that these as well as the other compositionally even more complex systems in the series have rice-ball structures. Interestingly, the photoelectron spectra of most of these are broad and essentially unstructured. It is difficult to make a general statement as to whether their spectral broadness indicates significant differences in the structures of their anions and their corresponding neutrals. This may also be due to multiple isomers present in the molecular beam. As rice-ball structures grow larger and presumably more globular, it seems unlikely that a difference of one electron between anions and their neutrals would induce major structural changes in so many different cluster systems. Moreover, photoelectron spectra often become broad and structure-less for large cluster anions just due to increasing spectral complexity.

In closing, we speculate as to why  $\text{Fe}_2\text{Bz}_3^-$ ,  $\text{Fe}_3\text{Bz}_3^-$ , and  $\text{Fe}_4\text{Bz}_4^-$  have enhanced ion intensities in the mass spectrum of the  $\text{Fe}_n\text{Bz}_m^-$  series.  $\text{Fe}_2\text{Bz}_3^-$  is the smallest cluster anion in this series to possess enough benzene molecules to form a stabilized rice-ball structure around an iron aggregate. This together with the fact that smaller clusters are often seen in greater abundance than larger ones, because it is kinetically easier to build-up smaller ones in the source's expansion, may be the reason why it is relatively abundant. While generally broad, the photoelectron spectrum of  $\text{Fe}_3\text{Bz}_3^-$  differs from the spectra of the other large cluster anions in that it has a peak at  $EBE = 1.7$  eV. One can imagine a high symmetry structure in which each benzene ring is attached to a corner of a  $\text{Fe}_3$  triangular core. Likewise, one is tempted to account for the enhanced ion intensity of  $\text{Fe}_4\text{Bz}_4^-$  by imaging a  $\text{Fe}_4$  tetrahedron core which is caged by four benzene molecules, each attached to one of its vertices.

#### Acknowledgments

This work was supported by the Division of Materials Science, Basic Energy Sciences, U.S. Department of Energy under Grant No. DE-FG02-95ER45538.

#### References

- [1] J.A. Crayston, J.N. Devine, J.C. Walton, *Tetrahedron* 56 (2000) 7829.
- [2] S. Ferlay, T. Mallah, R. Ouahes, P. Veillet, M. Verdager, *Nature* 378 (1995) 701.
- [3] J.S. Miller, A.J. Epstein, *Angew. Chem. Int. Ed.* 33 (1994) 385.
- [4] Y.M. Chen, P.B. Armentrout, *Chem. Phys. Lett.* 210 (1993) 123.
- [5] F. Meyer, F.A. Khan, P.B. Armentrout, *J. Am. Chem. Soc.* 117 (1995) 9740.
- [6] K.F. Willey, C.S. Yeh, D.L. Robbins, M.A. Duncan, *J. Phys. Chem.* 96 (1992) 9106.
- [7] M.A. Duncan, *Int. J. Mass Spectrom.* 272 (2008) 99.

- [8] T. Kurikawa et al., *Organometallics* 18 (1999) 1430.
- [9] T. Yasuie, A. Nakajima, S. Yabushita, K. Kaya, *J. Phys. Chem. A* 101 (1997) 5360.
- [10] T. Kurikawa, H. Takeda, A. Nakajima, K. Kaya, *Z. Phys. D* 40 (1997) 65.
- [11] M. Gerhards, O.C. Thomas, J.M. Nilles, W.J. Zheng, K.H. Bowen, *J. Chem. Phys.* 116 (2002) 10247.
- [12] K. Judai, M. Hirano, H. Kawamata, S. Yabushita, A. Nakajima, K. Kaya, *Chem. Phys. Lett.* 270 (1997) 23.
- [13] G. Luttgens, N. Pontius, C. Friedrich, R. Klingeler, P.S. Bechthold, M. Neeb, W. Eberhardt, *J. Chem. Phys.* 114 (2001) 8414.
- [14] W.J. Zheng, J.M. Nilles, O.C. Thomas, K.H. Bowen, *Chem. Phys. Lett.* 401 (2005) 266.
- [15] W.J. Zheng, J.M. Nilles, O.C. Thomas, K.H. Bowen, *J. Chem. Phys.* 122 (2005).
- [16] B.R. Sohnlein, D.-S. Yang, *J. Chem. Phys.* 124 (2006) 134305/1.
- [17] D. Rayane, A.R. Allouche, R. Antoine, M. Broyer, I. Compagnon, P. Dugourd, *Chem. Phys. Lett.* 375 (2003) 506.
- [18] C.W. Bauschlicher, H. Partridge, S.R. Langhoff, *J. Phys. Chem.* 96 (1992) 3273.
- [19] P. Chaquin, D. Costa, C. Lepetit, M. Che, *J. Phys. Chem. A* 105 (2001) 4541.
- [20] T.K. Dargel, R.H. Hertwig, W. Koch, *Mol. Phys.* 96 (1999) 583.
- [21] G.E. Froudakis, A.N. Andriotis, M. Menon, *Chem. Phys. Lett.* 350 (2001) 393.
- [22] B.K. Rao, P. Jena, *J. Chem. Phys.* 116 (2002) 1343.
- [23] B.K. Rao, P. Jena, *J. Chem. Phys.* 117 (2002) 5234.
- [24] R. Pandey, B.K. Rao, P. Jena, J.M. Newsam, *Chem. Phys. Lett.* 321 (2000) 142.
- [25] R. Pandey, B.K. Rao, P. Jena, M.A. Blanco, *J. Am. Chem. Soc.* 123 (2001) 3799.
- [26] T.D. Jaeger, D.V. Heijnsbergen, S.J. Klippenstein, G.V. Helden, G. Meijer, M.A. Duncan, *J. Am. Chem. Soc.* 126 (2004) 10981.
- [27] C.-N. Yang, S.J. Klippenstein, *J. Phys. Chem. A* 103 (1999) 1094.
- [28] O.C. Thomas, W.J. Zheng, K.H. Bowen, *J. Chem. Phys.* 114 (2001) 5514.
- [29] R.C. Bilodeau, M. Scheer, H.K. Haugen, *J. Phys. B* 31 (1998) 3885.
- [30] C. Adamo, V. Barone, *J. Chem. Phys.* 108 (1998) 664.
- [31] M.J. Frisch et al., *GAUSSIAN 03*. E01. Gaussian, Inc., Wallingford CT, 2004.
- [32] G.A. Zhurko, *Chem. Craft*. (<http://www.chemcraftprog.org>).
- [33] X. Li, S. Eustis, K.H. Bowen, A. Kandalam, *J. Chem. Phys.*, in press.